

Design and development of a controlled pressure/temperature set-up for *in situ* studies of solid–gas processes and reactions in a synchrotron X-ray powder diffraction station

Eduardo Salas-Colera,^{a,b} Álvaro Muñoz-Noval,^{a,b} Catherine Heyman,^c Conchi O. Ania,^d José B. Parra,^d Santiago García-Granda,^c Sofía Calero,^e Juan Rubio-Zuazo^{a,b} and Germán R. Castro^{a,b*}

^aSpLine, Spanish CRG BM25 Beamline, ESRF, 6 rue Jules Horowitz, 38000 Grenoble, France, ^bInstituto de Ciencia de Materiales de Madrid (ICMM, CSIC), Madrid, Spain, ^cCAO-DAO Heyman, 5 place de Gordes, 38000 Grenoble, France, ^dADPOR Group, Instituto Nacional del Carbón (INCAR, CSIC), Oviedo, Spain, and ^eDepartment of Physical, Chemical and Natural Systems, University Pablo de Olavide, Seville, Spain. *E-mail: castro@esrf.fr

A novel set-up has been designed and used for synchrotron radiation X-ray high-resolution powder diffraction (SR-HRPD) in transmission geometry (spinning capillary) for *in situ* solid–gas reactions and processes in an isobaric and isothermal environment. The pressure and temperature of the sample are controlled from 10^{-3} to 1000 mbar and from 80 to 1000 K, respectively. To test the capacities of this novel experimental set-up, structure deformation in the porous material zeolitic imidazole framework (ZIF-8) by gas adsorption at cryogenic temperature has been studied under isothermal and isobaric conditions. Direct structure deformations by the adsorption of Ar and N₂ gases have been observed *in situ*, demonstrating that this set-up is perfectly suitable for direct structural analysis under *in operando* conditions. The presented results prove the feasibility of this novel experimental station for the characterization in real time of solid–gas reactions and other solid–gas processes by SR-HRPD.

1. Introduction

Studying the properties of crystalline materials requires the development of very sophisticated characterization techniques. High-resolution powder X-ray diffraction (HRPD) is one of the most widely exploited characterization techniques for crystalline materials due to its experimental simplicity and the large amount of information that it provides (Lipson & Steeple, 1970). Using synchrotron sources for these diffraction techniques is required in order to obtain higher resolution and larger incident fluxes with the aim to be able to study the shortest changes in samples in shorter collecting times. Moreover, the sensitivity of the structure to the X-ray diffraction technique was incredibly boosted by the development of new-generation synchrotron sources and the creation of specialized experimental stations (Roberts, 1993; Hastings *et al.*, 1984; Ferrer *et al.*, 2012, 2013). The study of crystalline structure in materials during complex processes requires on some occasions the development of the experimental set-up and equipment with a controlled experimental environment (Cernik *et al.*, 1995; Hannemann *et al.*, 2007; Ihringer & Küster, 1993), which may provide control of the macroscopic

properties (*i.e.* temperature or pressure) that can influence the microscopic properties of crystalline materials.

For synchrotron X-ray powder diffraction experiments in transmission geometry using a capillary, inherent difficulties arise from the experimental configuration of the instruments and the nature of the samples. The powder sample is placed inside a capillary (*i.e.* quartz or borosilicate) and the capillary is spun perpendicular to the X-ray beam to avoid observation of the diffraction in a preferred crystallographic direction. The possibility to manage the sample environment and to keep such a capillary spinning, most of which are less than 0.5 mm in diameter, is a difficult challenge. These capillaries are also very delicate, making sample manipulation difficult. This, therefore, makes measuring under non-standard pressure conditions difficult, and most experiments are carried out at atmospheric or in an air-thick capillary with preset conditions.

Zeolitic imidazole frameworks are a class of metal-organic frameworks composed of tetrahedral networks of bivalent transition metals (Zn, Co, Cu) linked by the organic methyl-imidazole (CH₂N(NH)CH₃) ligand. These large porous crystalline materials are structured with great stability (Park *et al.*, 2006) under different environmental conditions. These mate-

rials are used to capture and store several types of gases such as CO₂, N₂ and CH₄ (Banerjee *et al.*, 2008; Hayashi *et al.*, 2007). They are used to develop gas adsorption systems for catalytic and gas-trapping applications. The structural modifications and adsorption mechanisms during the adsorption processes are not yet well understood and are a key issue to comprehend the nature of this family of materials. In this sense the possibility to eventually study *in situ* structural modifications might be a milestone to determine the gas adsorption mechanisms in this family of materials. In this sense, SR-HRPD becomes a necessary tool for obtaining new clues about these systems.

A high-resolution gas adsorption/desorption isotherms experiment in the zeolitic imidazole framework (ZIF-8) material was carried out previously (Ania *et al.*, 2012), in which a selected set of gases (Ar, N₂, O₂ and CO) were chosen due to their distinctive molecular properties (*i.e.* polarizability, size, shape, *etc.*). The adsorption/desorption isotherms measured at a cryogenic temperature of 77 K show three very different regions as a function of gas pressure. Molecular simulations studies on the crystallographic structure of ZIF-8 materials cannot completely explain the adsorption/desorption behaviour. Therefore, it has become necessary to develop an experimental set-up suitable for studying the structural properties of ZIF-8 material under gas adsorption conditions in order to elucidate the gas adsorption/desorption phase transition observed.

In this paper we present the design, development and commissioning of a novel versatile spinning-sample set-up for performing experiments under isothermal and isobaric conditions at controlled gas atmospheres, which enable spinning the sample in transmission-mode SR-HRPD experiments. Herein, as an example, we show a preliminary result of the structural properties of ZIF-8 material using SR-HRPD measurements to elucidate the enumerate problems. Powder diffraction measurements were carried out at different Ar and N₂ gas pressures under isothermal and isobaric conditions. The main innovations for the cell presented in this work are the fact that it can, under isothermal and isobaric conditions, characterize the solid–gas process keeping the powder sample spinning and enable the simultaneous acquisition of SR-HRPD data. The set-up permits accurate control of the sample temperature and pressure in the range 80–1000 K and 10^{−3}–1000 mbar, respectively. The diffraction method for characterizing the gas adsorption properties is more sensitive and convenient compared with some of the more conventional techniques and can provide additional information when structural modification takes place.

2. Experimental set-up

Branch A of the Spanish CRG BM25-SpLine beamline at the European Synchrotron Radiation Facility (ESRF) has been designed as a multipurpose beamline (Rubio-Zuazo & Castro, 2009) where both X-ray absorption spectroscopy (XAS) and HRPD experiments can be carried out. Branch A of SpLine is located on the soft edge of the D25 bending magnet with a

critical energy of 9.7 keV. Horizontally it accepts 2 mrad of the beam delivered by the D25 dipole. The spot size can be changed between 12 mm × 8 mm (H × V) and 0.3 mm × 0.1 mm. SR-HRPD measurements can be performed within a photon energy range of 5–45 keV (2.48–0.35 Å wavelength range) with an energy resolution of $\Delta E/E = 10^{-4}$ (Rubio-Zuazo *et al.*, 2013; Castro, 1998). Hence, *K*- and *L*-edge resonance experiments can be performed together with non-resonance experiments. The HRPD station shares the experimental hutch and optics with the X-ray absorption station of the SpLine branch A beamline. The use of the SR-HRPD station is coordinated with the use of beam time on the XAS station. Both stations cannot be offered simultaneously. The HRPD set-up is installed at ~45 m from the source. The heavy-duty θ – 2θ diffractometer is placed at a distance of 1000 mm from the centre to the detector and it has a central passage of 290 mm suitable for equipment for studying samples in different environments, *i.e.* reactions cells, ovens and cryostats, *etc.* The detector arm is rigid enough to accept heavy detectors (~50 kg). The angular resolution for the detector movement is better than 10^{−5} degrees. The main axis for the θ and 2θ circles is the horizontal axis, such that diffraction measurements are performed in the vertical plane. Under this condition it is possible to take advantage of the high polarization degree of synchrotron radiation. Samples can be accommodated either in a flat plate or in capillaries of different diameter according to the sample absorption properties and the amount of sample available. Details of the powder diffraction station are shown in Fig. 1. The home-designed θ – 2θ diffractometer features a custom-designed multi-crystal detector stage. This stage incorporates ten single point-detectors [NaI(Tl) scintillation] operated in parallel and each point-detector is equipped with a Ge(111) single-crystal analyzer in a θ – 2θ configuration. The diffractometer, which is manufactured by HUBER GmbH, can be used in reflection and transmission (thin films and capillary) configurations. Both the diffractometer and the multi-analyzer detector set-up produce a significant resolution improvement on the

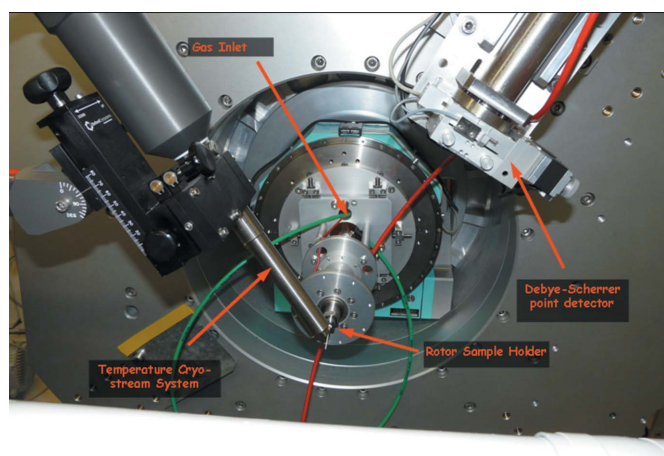


Figure 1
Frontal view of the diffractometer and experimental set-up.

powder diffraction station, keeping a relatively low acquisition time, since simultaneous parallel detection (ten channels) is accomplished. The total angular resolution is better than 0.01° FWHM. The experimental station is additionally equipped with a NaI(Tl) point scintillation detector in Debye–Scherrer geometry. The active surface has a diameter of 30 mm and a collimating rectangular pipe of $10\text{ mm} \times 20\text{ mm} \times 100\text{ mm}$. This detector set-up includes three two-axis slits set-ups: the first one before the sample (pre-sample slits) and the other two set as anti-scatter slits and detector slits just before the point detector. Diffractometer alignment is achieved by using stages for three degrees of freedom. Two of them are used for translation in the x and z directions (z is the vertical direction and x is perpendicular to the X-ray beam). The other stage is used for a rotation motion around the X-ray beam, in order to tilt the diffractometer to assure the optimal detection geometry, *i.e.* the detector forms an angle of 90° with respect to the X-ray electrical polarization vector. The whole device is mounted on a rail system which allows the diffractometer to be moved back to keep enough clear space for easy mounting and dismounting of sample environments and/or detector systems. An ionization chamber is placed between the pre-sample slits and the sample in order to quantify the incident beam intensity to normalize the diffraction pattern measured. The sample can be cooled down to 80 K by means of a liquid-nitrogen open-flow cooler, series 700 from Oxford Cryostream, and also heated up to 1000 K using an external hot-air blower commercialized by Cyberstar, France. Both components cannot work together and they do not interfere with the detector movement. The Oxford Cryostream cooler system can work in a temperature range from 80 to 400 K. Hence, *in situ* sample thermal treatment can be performed.

During the present experiment, the X-ray beam wavelength was set to 0.772939 \AA in order to make a compromise between the maximum diffraction signal and minimum absorption in the samples. The beam spot size was set at $4\text{ mm} \times 1\text{ mm}$ to ensure homogeneous conditions of temperature in the beam path across the sample mounted in a capillary. Standard Reference Material (SRM) 640c Si powder from the National Institute of Standards and Technology (NIST) was used for calibrating the wavelength and temperature and to align the diffractometer. The powder Si reference was mounted in a 0.5 mm quartz capillary. Quartz capillaries of the same diameter were used for placing all the samples in this experiment. Temperature calibration was performed by fitting the thermal expansion/contraction of eight diffraction peaks of the Si reference with the thermal expansion coefficient. During the isothermal experiments the diffraction patterns were acquired at 85 K, with a temperature error of 1 K. Both temperature and pressure were remotely monitored in order to maintain an isothermal and isobaric reactive environment in the sample during each scan. At each of the selected experimental working conditions a diffraction pattern was obtained in the 2θ range from 3° to 65° corresponding to a resolution of better than 0.7 \AA . The diffraction patterns were acquired with an angular step of 0.02° and an integration time of 5 s.

2.1. Rotation sample holder

One of the novel elements of this experimental set-up is the home-designed rotation sample holder. Normally, in powder diffraction experiments carried out in transmission mode the samples are contained in capillaries of different diameters. The capillaries are required to rotate during data acquisition in order to avoid preferential crystallographic orientations in the diffraction pattern measured. Fig. 1 shows a photograph of the designed set-up mounted in the SR-HRPD diffractometer. The novel rotation sample holder system has been designed to manage *in situ* the gas atmosphere and pressure environment in the sample; meanwhile the capillary keeps spinning during the powder diffraction experiments. The rotation sample holder is composed of three main parts: the shaft-rotor, which holds the capillary support sample holder pipe; the rotary union, which connects the rotating part with the pump/gas-supplier system; and the support table, which keeps the capillary aligned. Fig. 2 shows schema of the rotation sample holder. The shaft-rotor, which has a central conic hole throughout to receive the sample holder pipe, is mounted between two pre-load high-precision angular contact ball-bearings. A washer and a nut placed on the end of the shaft tighten the sample holder pipe into the bearing races. The bearing distance is 100 mm and its critical shaft speed is 19000 r.p.m. The rotation is transmitted by a two-gear system (module 0.5, 40/30 ratio) and a DC motor. The rotation speed is controlled by the applied voltage. The actual capillary sample holder pipe has a pumping hole throughout, a conical end for centring and a VCR connector. The sample holder is mounted on the rotation shaft by means of a washer and a nut. The conical end assures the centring of the capillary with respect to the rotation axis. The VCR connector on the other side is connected to the rotary union and pumping system. The sample holder possesses a conical receptacle [see Figs. 2(a) and 2(b)] for placing the conical cases where the copper sample holders are mounted. Finally, a holey nut closes the rotor head and seals the system. The rotary union is connected by a flexible hose to the sample holder pipe. The sample holder pipe has anti-rotation slits where a key is allocated to be fixed on the rotation shaft. The rotary union is home-designed and consists of an external housing and a central shaft, two sealed ball-bearings and two dynamic seals, all of them mounted using a retaining ring in a compact design (see Fig. 2c). The rotary union enables the union between the gas-supplier/pump-system and the rotating capillary. A sealing system between the static head and rotor head keeps the inner atmosphere controlled and isolated from the room atmosphere. In order to guarantee homogeneous spinning, the shaft-rotor and the sample-holder pipe are made of stainless steel, with outer diameter 25 mm. The axial inertial moment of the rotating assembly is about 1200 kg mm^{-2} . This design allows the capillary to be spun at a constant velocity during the SR-HRPD acquisition. The axis wobble or angular deviation of the axis is less than 0.005° . The shaft-rotor is mounted on a translation table with four degrees of freedom for precise alignment of the capillary in the diffractometer centre.

This set-up has been designed to fit with the heavy-duty home-designed diffractometer of BM25-Spline, taking advantage of the exceptional experimental set-up. However, it could be universally adapted to any standard powder diffraction station.

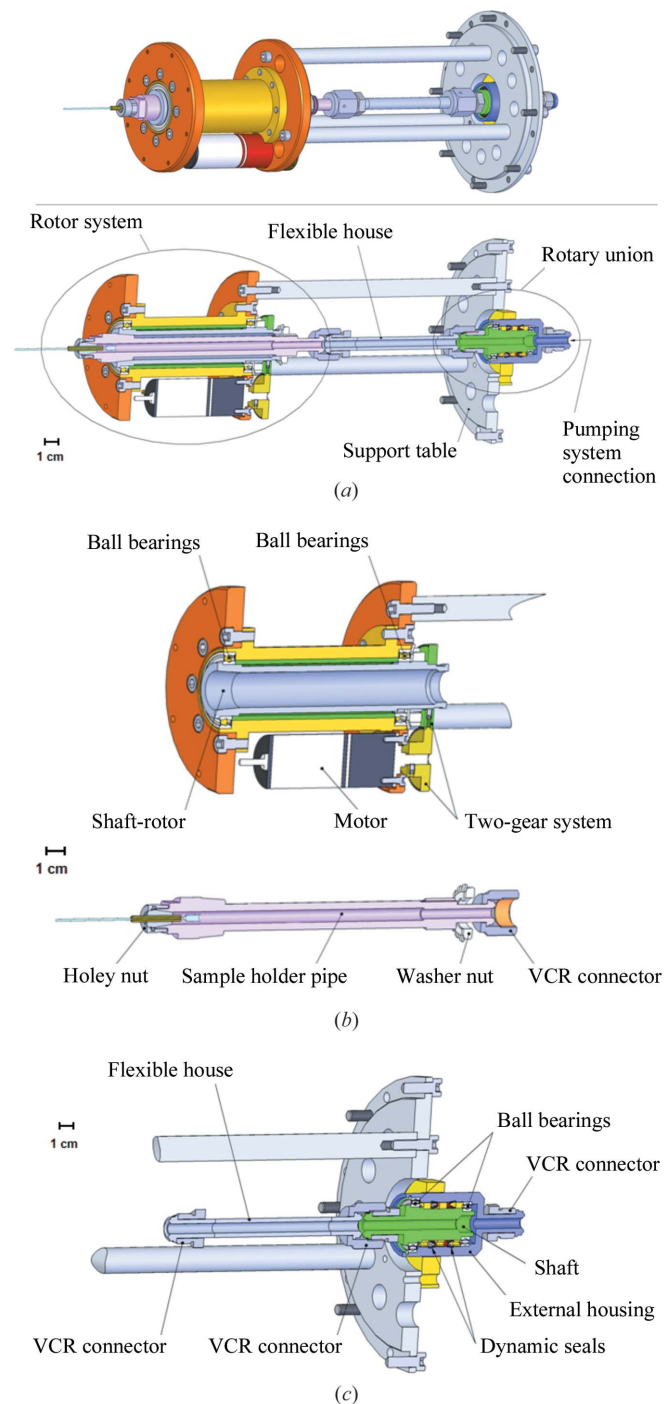


Figure 2
 (a) Scheme of the rotation sample holder. The three main elements of this device are pointed out: on the left the rotor system, in the middle the flexible house, and on the right the rotary union. (b) Scheme of the shaft rotor. For clarity the expanded/dismount part are presented: top, shaft-rotor; bottom, capillary support sample holder pipe. The different components are shown (see text). (c) Scheme of the rotary union. The different components are shown (see text).

2.2. Gas system

The main goal of this novel experimental add-on is the possibility to carry out powder diffraction measurements under isobaric and isothermal working conditions using any kind of gas or mix of gases. At this point it is necessary to point out that temperature variances produce changes in the gas pressure as the thermodynamic equilibrium forces the inner gas to compress or to expand. Moreover, in a closed rotating system, as usually used in powder diffraction, gas leaks could produce changes in gas pressure; furthermore, it is necessary to consider that obtaining a complete diffractogram could take a few hours. Thus, in a closed system it is not possible to perform isobaric measurements under standard conditions. Therefore, the gas pressure in the system is managed by controlling/coordinating the gas inlet and gas outlet rates. Thus, it is possible to produce a quasi open system with a controlled and stable gas atmosphere during the required time of measurement. Gas inlet and outlet are controlled by means of independent mass flow controllers which enable a precise setting of the gas pressure in the capillary. In a similar way, the gas pressure inside can be increased or decreased by adjusting the blow/exhaust flux imbalance. That is how we have achieved combining the air-thick rotor sample holder system with a controlled pressure and composition gas environment at the sample. The set-up can work in the pressure range from 10^{-3} to 1000 mbar. The gas flow assembly scheme is summarized in Fig. 3. Coming from the sealed static head, the gas tube is connected to a capacitive pressure gauge meter that is placed close to the sample to obtain correct pressure measurement. From here there are two tracks: one coming from the gas supplier and the other going to the gas exhaust, each one managed by a four-channel mass flow controller and their respective control electronics (models 5850S/BC, Brooks Instruments). The gas supplier is connected to a four-channel gas station which enables four different kinds of inlet gases (each of them can reach 50 sccm) to be combined. A third track is connected straight to an oil-free rotary pump that is used to achieve a negative pressure difference (down to 10^{-3} mbar) with the exhaust for reaching a pressure equilibrium and, eventually, evacuate the gas. In this case it is possible to evacuate at a maximum rate of 200 sccm under standard conditions. Both the incoming and outgoing streams are controlled by the electronic valve system.

3. HRPD measurements under controlled atmosphere conditions

As an example of the feasibility of this set-up to perform isothermal and isobaric experiments, we carried out a study of the gas-induced structural deformation of the zeolitic imidazole framework (ZIF-8) system. It is important to stress that it is not our goal in this work to explain the structural evolution during the isothermal study. The structural interpretation is the object of a more exhaustive study which is in preparation and will be presented in a second work. Following previous results for this kind of structure (Banerjee *et al.*, 2008), an

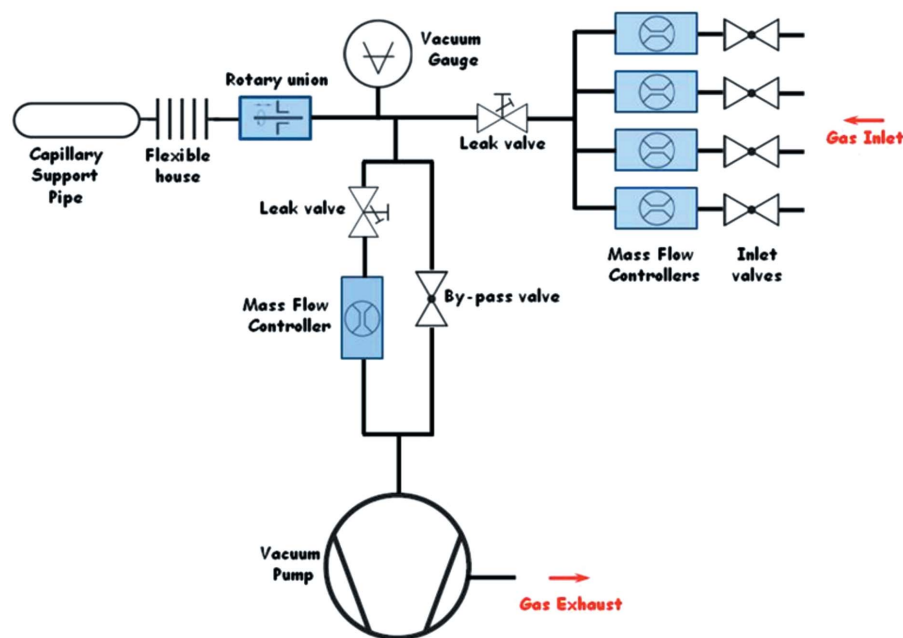


Figure 3
Scheme of the gas inlet and gas exhaust system used to perform the isobaric/isothermal experiments. For clarity, only the main elements are displayed.

exhaustive *in situ* study was required in order to clarify the mechanism of the gas adsorption process under isothermal conditions. In this experiment, diffraction patterns of the ZIF-8 sample were acquired at different gas pressure and temperatures, keeping isobaric and isothermal working conditions during data acquisition. In the current study, Ar and N₂ gases were used to induce the deformation mechanism in the ZIF-8 network. In order to obtain a structural reference of the initial state of the sample, a diffraction pattern of the ZIF-8 sample was measured at high vacuum (10⁻³ mbar). Then, the reaction gas was dosed into the sample at a pre-

selected pressure. The SR-HRPD data were measured in the 2θ range 3–65° corresponding to a resolution better than 0.7 Å. Fig. 4(a) shows the diffraction patterns of ZIF-8 measured at 85 K with N₂ atmosphere within a range of pressures from vacuum (10⁻³ mbar) to 325 mbar. For clarity, the diffractograms are shown only in the 2θ range 3–29°. Within this pressure range noticeable changes in the diffractograms were observed for both systems. In the case of the isothermal adsorption experiments performed with Ar, the pressure ranged from 14 to 568 mbar at the same temperature of 85 K (not shown). Fig. 4(b) shows a blow-up (2θ range 7–16°) of the data obtained at an N₂ pressure of 325 mbar (top diffractogram in red) and at 10⁻³ mbar (bottom diffractogram in black). The arrows show the most visible changes. The most impressive feature that can be noted is the appearance of a new diffraction

peak at 2θ = 10.42° when the N₂ or Ar (not shown) pressure increased. The intensity of this new peak increases as the N₂ pressure rises to the top value. Similar changes and behaviour in the diffraction pattern were observed as a function of Ar pressure. In both cases, *i.e.* N₂ and Ar gas adsorption at 85 K, the changes obtained in the previous isotherms experiment (Ania *et al.*, 2012) can be correlated with structural changes observed by SR-HRPD and can be explained by the effect of structural deformation in the porous structure of the ZIF-8 system due to gas adsorption. For both gases the intensity of the diffraction peak at 10.42° increases when the gas pressure

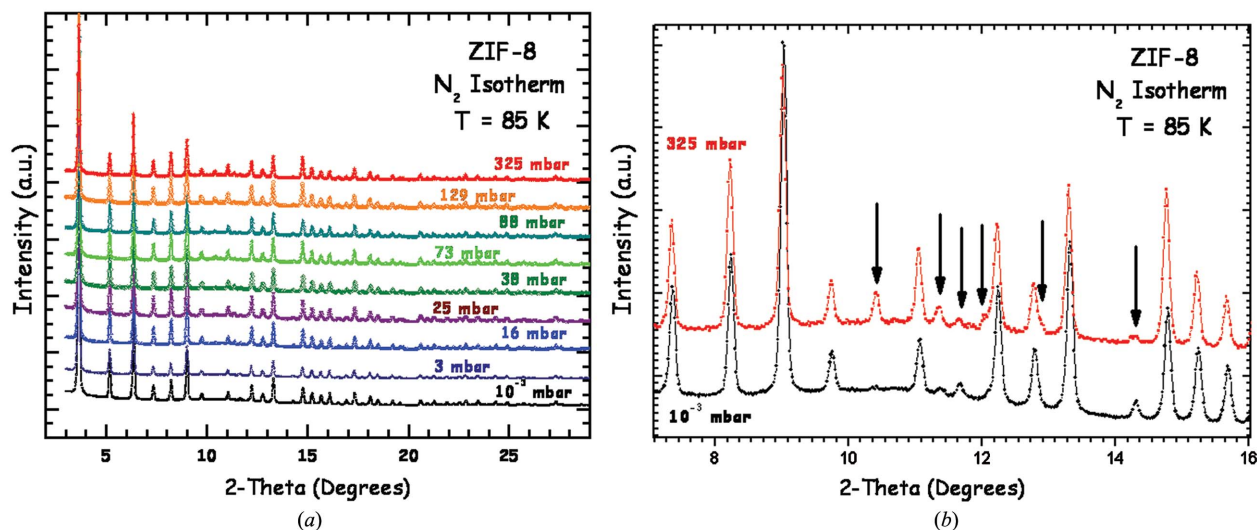


Figure 4
(a) Partial diffractograms (3–28°) of the ZIF-8 isothermal gas adsorption experiments carried out in N₂ atmosphere at 85 K and different gas pressures. The X-ray beam wavelength was set to 0.772939 Å. (b) Diffractogram blow-up (7–16° 2θ) for two N₂ equilibrium pressures: saturation 325 mbar (top, red) and vacuum (bottom, black). The vertical arrows point to the most relevant diffractogram changes. The X-ray beam wavelength was set to 0.772939 Å.

rises. The peak intensity was obtained by means of a pseudo-Voigt function fitting. The peak intensity evolution follows quite well the volumetric isotherm evolution [see Figs. 5(a) and 5(b) and text below]. The SR-HRPD data have characteristic features in each different region of the isotherm and its dependence on the pressure is increased or reduced. Figs. 5(a) and 5(b) show the intensity evolution of the 10.42° diffraction peak as a function of the of N₂ and Ar equilibrium pressure, respectively. The intensity corresponding to 325 mbar for N₂ and 568 mbar for Ar has been normalized to unity. For comparison, high-resolution adsorption isotherms for both gases [N₂ (Fig. 5a) and Ar (Fig. 5b)] are shown. The numbers in the diffraction intensity data correspond to the

adsorption sequence. The inset in both figures shows, as an example, four expanded (8.5–11.5°) diffractograms at different gas pressure; the arrows point to the corresponding region in the isotherm. The intensity evolution shows a good correlation with the adsorption isotherms obtained separately by volumetric methods. Both experiments, with Ar and N₂, are summarized in Fig. 5 in which the diffractograms were acquired at a constant temperature of 85 K and varying the gas pressure in the sample within the pressure range where the structural phase transition is expected to occur.

As demonstrated in previous papers, this structural deformation depends on the molecular properties of the guest gas (*i.e.* polarizability, size and shape, *etc.*) (Ania *et al.*, 2012).

Nevertheless, the study of this kind of ZIF-8 system and the mechanisms involved in the transitions produced by the gas adsorption will require further work in the analysis of the presented results.

4. Conclusions

In this paper we have reported the design, development and performance of a novel experimental system that allows the *in situ* structural characterization of solid–gas processes by means of SR-HRPD at the powder diffraction station of the Spanish CRG BM25-SpLine at the ESRF. This novel set-up allows the study of *in situ* gas adsorption and solid–gas reactions under isobaric and isothermal working conditions. With the current capabilities the temperature ranges from 80 to 1000 K and the pressure ranges from 10^{−3} to 1000 mbar, keeping the capillary spinning. This novel system has been designed to be exploited in powder diffraction experiments at the Spanish CRG BM25-SpLine beamline at ESRF but could be universally adapted to a standard powder diffraction station. The feasibility of the experimental system has been tested and demonstrated in the study of low-temperature isothermal experiments to prove the gas-induced deformation in a zeolitic imidazole framework, a zeolite-type porous material. During this test it has been possible to observe direct structural phase transitions. The observed changes have been attributed to isothermal gas adsorption by the porous structure. Thus, this novel set-up has demonstrated to be a useful tool for the

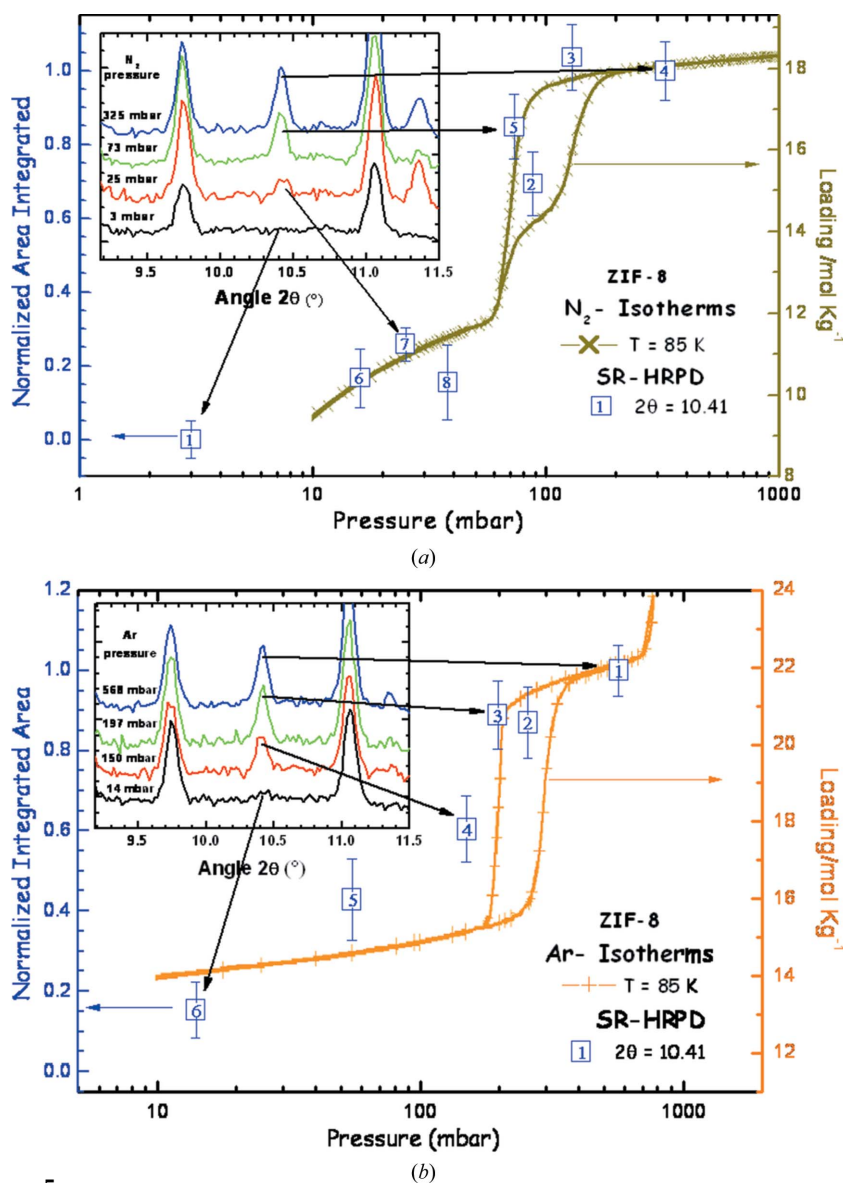


Figure 5

(a) N₂ ZIF-8 isothermal gas adsorption experiments carried out at 85 K and different N₂ pressures. The inset shows details of the region in which one of the most characteristic peaks of the adsorption process appears. The numbers in the diffraction data correspond to the sequence of gas dosing in the adsorption branch. (b) Ar ZIF-8 isothermal gas adsorption experiments carried out at 85 K and different Ar pressures. The inset shows four examples of details of the regions in which the used peaks of the adsorption process appear. The numbers in the diffraction data correspond to the sequence of gas dosing in the adsorption branch.

in situ study of these and other kinds of solid–gas processes by SR-HRPD.

The authors are grateful to the SpLine staff for their assistance. Financial support under grant PIE 201060E013 of the Consejo Superior de Investigaciones Científicas-CSIC and the Spanish Ministry of Economy and Competitiveness MINECO is also acknowledged.

References

- Ania, C. O., García-Pérez, E., Haro, M., Gutiérrez-Sevillano, J. J., Valdés-Solís, T., Parra, J. B. & Calero, S. (2012). *J. Phys. Chem. Lett.* **3**, 1159–1164.
- Banerjee, R., Phan, A., Wang, B., Knobler, C., Furukawa, H., O’Keeffe, M. & Yaghi, O. M. (2008). *Science*, **319**, 939–943.
- Castro, G. R. (1998). *J. Synchrotron Rad.* **5**, 657–660.
- Cernik, R. J., Craig, S. R., Roberts, K. J. & Sherwood, J. N. (1995). *J. Appl. Cryst.* **28**, 651–653.
- Ferrer, P., da Silva, I., Heyman, C., Rubio-Zuazo, J. & Castro, G. R. (2013). *J. Phys. Conf. Ser.* **425**, 132001.
- Ferrer, P., da Silva, I., Rubio-Zuazo, J., Alfonso, B. F., Trobajo, C., Khainakov, S., Garcia, J. R., Garcia-Granda, S. & Castro, G. R. (2012). *J. Synchrotron Rad.* **19**, 93–100.
- Hannemann, S., Casapu, M., Grunwaldt, J.-D., Haider, P., Trüssel, P., Baiker, A. & Welter, E. (2007). *J. Synchrotron Rad.* **14**, 345–354.
- Hastings, J. B., Thomlinson, W. & Cox, D. E. (1984). *J. Appl. Cryst.* **17**, 85–95.
- Hayashi, H., Côté, A. P., Furukawa, H., O’Keeffe, M. & Yaghi, O. M. (2007). *Nat. Mater.* **6**, 501–506.
- Ihringer, J. & Küster, A. (1993). *J. Appl. Cryst.* **26**, 135–137.
- Lipson, H. & Steeple, H. (1970). *Interpretation of X-ray Powder Diffraction Patterns*. London: McMillan.
- Park, K. S., Ni, Z., Côté, A. P., Choi, J. Y., Huang, R., Uribe-Romo, F. J., Chae, H. K., O’Keeffe, M. & Yaghi, O. M. (2006). *Proc. Natl Acad. Sci.* **103**, 10186–10191.
- Roberts, K. J. (1993). *J. Cryst. Growth*, **130**, 657–681.
- Rubio-Zuazo, J. & Castro, G. R. (2009). *Semin. Soc. Esp. Mineral.* **6**, 89–108.
- Rubio-Zuazo, J., Collado-Negro, V., Heyman, C., Ferrer, P., da Silva, I., Gallastegui, J. A., Gutiérrez-León, A. & Castro, G. R. (2013). *J. Phys. Conf. Ser.* **425**, 052005.